

Supplementary material: A stochastic reaction diffusion modeling investigation of FLASH ultra-high dose rate response in different tissues

Ramin Abolfath^{1,2,†}, Alexander Baikalov^{3,4}, Alberto Fraile⁵, Stefan Bartzsch^{3,6}, Emil Schüler¹, Radhe Mohan¹

¹ Department of Radiation Physics and Oncology,
University of Texas MD Anderson Cancer Center, Houston, TX, 75031, USA

² Physics Department, Sharif University of Technology,
P.O.Box 11365-9161, Azadi Avenue, Tehran, Iran

³ Technical University of Munich, Department of Physics, Garching, Germany

⁴ Helmholtz Zentrum München GmbH, German Research Center for Environmental Health,
Institute of Radiation Medicine, Neuherberg, Germany

⁵ Nuclear Futures Institute, Bangor University, Dean Street, Bangor, LL57 2DG, United Kingdom

⁶ Technical University of Munich, School of Medicine and Klinikum rechts der Isar,
Department of Radiation Oncology, Munich, Germany

(Dated: April 24, 2023)

PACS numbers:

I. SUPPLEMENTARY MATERIAL

A. Semi-analytical approach to a system of single tracks

The rate equations proposed in this work describe reactive oxygen species (ROS) aggregation and formation of non-reactive oxygen species (NROS) agglomerates such as transformation of a pair of $\cdot\text{OH}$ to stable compounds such as H_2O_2 or transient and metastable complexes of $\cdot\text{OH}\cdots\cdot\text{OH}$. We introduce two dynamical variables $u(\vec{r}, t)$ and $v(\vec{r}, t)$ and propose a system of coupled reaction-diffusion equations, denoting $u = [\cdot\text{OH}]$ and $v = [\text{H}_2\text{O}_2]$. These variables represent fast (ROS) and slow (NROS) moving species.

Conversion of ROS ($\cdot\text{OH}$) to NROS (H_2O_2) and vice versa can be described by the following rate equations

$$\frac{\partial u}{\partial t} = G + \vec{\nabla} \cdot (D_f(\vec{r})\vec{\nabla}u) - k_1u + k_2v - 2k_3u^2 - k_{12}uv, \quad (1)$$

$$\frac{\partial v}{\partial t} = k_1u - k_2v + k_3u^2. \quad (2)$$

Here $G(\vec{r}, t)$ and D_f represent the dose rate and diffusion constant of the fast moving species (neglecting the diffusion of slow moving species), and k_1, k_2, k_3, k_{12} are reaction rate constants.

For a homogenous and uniform system, D_f is a constant, hence in Eq. (1) we can substitute $D_f\nabla^2u$ for $\nabla \cdot (D_f(\vec{r})\nabla u)$. In the following, we calculate analytical solutions of Eqs. (1) and (2), considering D_f a constant. However, for random networks considered in this work, D_f is a function of position, \vec{r} . In this case we calculate solutions of Eqs. (1) and (2) numerically.

Eqs. (1) and (2) are generalizations of ROS-NROS rate equations introduced by Eqs.(1) and (2), in Ref. [1], where the “non-linearities” in the rate equations have shown the dominance of NROS at UHDRs. Note that in

the current work, we have added thermal diffusion and steady state decay terms (k_1 and k_2) where in the absence of linear terms, $D_f = k_1 = k_2 = 0$, we can recover Eqs. (1) and (2) in Ref. [1] (after substituting the variables N_1 and N_2 for u and v).

The numerical values of the rate constants are available in MC codes such as TOPAS n-Bio [2], used in our related recent study [3]. For example, the reaction rate constant of $\cdot\text{OH} + \text{H}_2\text{O}_2 \rightarrow \cdot\text{HO}_2 + \text{H}_2\text{O}$ is given by $k_{12} = 0.0023 \times 10^{10}/M/s = 0.023/M/ns$. Similarly the reaction rate constant of $\cdot\text{OH} + \cdot\text{OH} \rightarrow \text{H}_2\text{O}_2$, described by Eq. (2), $d[\text{H}_2\text{O}_2]/dt = k_3[\cdot\text{OH}]^2$, is $k_3 = 0.475 \times 10^{10}/M/s = 4.75/M/ns$. In the absence of non-linearities ($k_3 = k_{12} = 0$) and zero diffusion, the linear rate constants, k_1 and k_2 , can be determined from a steady-state condition where u and v are both constant so $du/dt = dv/dt = 0$, thus $v = (k_1/k_2)u$ where $G = 0$.

With regards to differences with our latest work, presented in Ref. [3], we have omitted the labels for the track indices in u and v as the explicit inclusion of indices is convenient for the description of weak inter-track limit where the analytical solutions and the overlap integrals can be calculated perturbatively. Nevertheless, to recover the rate equations in Ref. [3], we apply the following transformation $u = \sum_{i=1}^{N_s} u_i$ in Eq. (1) where N_s denotes the number of particle tracks, identical to the number of particles in a beam. Substituting this transformation results in partitioning Eq. (1) into N_s independent rate equations. A one-to-one correspondence between the variables in this model and in Ref. [3] is the following: $u_i \rightarrow c_i$, $D_f \rightarrow \alpha$, $k_1 \rightarrow k_s$ and $2k_3 \rightarrow k_r$. The rest of the parameters and variables, k_2, k_{12} and v were omitted in Ref. [3].

Therefore, the rate equations presented in the current study, Eqs. (1) and (2), are more general than their counterparts in Ref. [3] and the solutions at the limit of weakly and/or strongly correlated tracks can be calculated non-perturbatively by numerical approaches such as finite difference and/or elements.

An interesting special limiting case of negligible k_1, k_2 ,

k_3 , and k_{12} corresponds to an asymptotic solution of the Gaussian distribution function for u at $t \gg 0$ as studied in Ref. [3]. Note that we use slightly different initial conditions such that at $t = 0$ a constant distribution of ROS inside a cylinder with radius w is considered, where $u = u_0$ within $r \leq w$ and zero otherwise, and $v = v_0 = 0$ everywhere. w is the width of a particle track at initial time $t = 0$ and it can be extracted from MC simulations of track structures of particles. w is a parameter that depends on particle LET. The advantage of using this initial condition would be omission of parameter τ_0 introduced in Ref. [3] in favor of the initial track width w . Geometrically, tracks with this boundary condition do not suffer from a spurious Gaussian tail at initial time.

At the weak interaction limit we disregard the non-linear terms to calculate analytical solutions. We further treat the non-linear terms perturbatively and calculate the corrections to linear solutions. Note that the analytical solutions at the strong limit of non-linearities have been calculated in Ref.[1]. Thus, we may perform an interpolation between weak and strong interaction limits to calculate the solutions at the intermediate interacting limit where both linear and non-linear terms are comparable. The rest of this presentation is devoted to calculating the solutions of these equations.

To handle the time dependence in the partial differential equations we perform a Laplace transformation

$$\bar{u}(s, \vec{r}) = \int_0^\infty dt u(\vec{r}, t) e^{-st}, \quad (3)$$

with the inverse Laplace transformation, given by

$$u(\vec{r}, t) = \frac{1}{2\pi i} \int_{\gamma-i\infty}^{\gamma+i\infty} dp \bar{u}(s, \vec{r}) e^{st}. \quad (4)$$

Insertion of Eq. (3) to the time-derivative term in Eqs. (1) and (2) yields

$$\int_0^\infty dt \frac{\partial u(\vec{r}, t)}{\partial t} e^{-st} = -u(0, \vec{r}) + s\bar{u}(s, \vec{r}), \quad (5)$$

where $u(0, \vec{r})$ can be specified by the initial condition for u at $t = 0$, $u(0, \vec{r}) = u_0(\vec{r})$. Linearizing the rate equations and applying the Laplace transformation, we treat the non-linear terms perturbatively

$$\begin{aligned} s\bar{u}(s, \vec{r}) &= \bar{G}(s) + D_f \nabla^2 \bar{u}(s, \vec{r}) \\ &- k_1 \bar{u}(s, \vec{r}) + k_2 \bar{v}(s, \vec{r}) + u(0, \vec{r}) \end{aligned} \quad (6)$$

and

$$\bar{v}(s, \vec{r}) = \frac{k_1 \bar{u}(s, \vec{r}) + \bar{v}(0, \vec{r})}{s + k_2} \quad (7)$$

We can now replace Eq.(7) in Eq.(6) and reduce the system of coupled differential equations into a single equation in terms of u , thus

$$\begin{aligned} \nabla^2 \bar{u}(s, \vec{r}) &- q^2 \bar{u}(s, \vec{r}) = \\ &- \frac{1}{D_f} \left[\frac{k_2 \bar{v}(0, \vec{r})}{s + k_2} + (\bar{G} + \bar{u}(0, \vec{r})) \right] \end{aligned} \quad (8)$$

where

$$q^2(s) = \frac{s}{D_f} \left(1 + \frac{k_1}{s + k_2} \right). \quad (9)$$

Applying the initial conditions everywhere

$$u(0, \vec{r}) = v(0, \vec{r}) = 0 \quad (10)$$

we find

$$\nabla^2 \bar{u}(s, \vec{r}) - q^2 \bar{u}(s, \vec{r}) = -\bar{G} \quad (11)$$

Alternatively, we can start the time-evolution of the track expansion by applying the initial conditions right after entrance of the single track where we can consider $G = 0$, from that time on. Here the track structure insertion to the differential equations can be performed through the boundary conditions $u(t = 0, \vec{r}) = u_0 \theta(w - r)$, and $v(t = 0, \vec{r}) = v_0 \theta(w - r)$, hence Eq. (8) simplifies to

$$\nabla^2 \bar{u}(s, \vec{r}) - q^2 \bar{u}(s, \vec{r}) = -V(s) \theta(w - r), \quad (12)$$

where

$$V(s) = \frac{u_0}{D_f} \left[1 + \frac{k_2}{s + k_2} \frac{v_0}{u_0} \right]. \quad (13)$$

Here $\theta(w - r)$ is a Heavyside function such that $\theta = 1$ if $r \leq w$ and zero, otherwise. Eq. (12) is of the general form given in Carslaw and Jaeger [4] for heat conduction between composite cylinders. For $r \leq w$ the solutions of Eq. (12) are

$$\bar{u}_<(s, \vec{r}) = \frac{V}{q^2} - \alpha_1(s) I_0(qr), \quad (14)$$

$$\bar{v}_<(s, \vec{r}) = \frac{k_1}{s + k_2} \bar{u}_<(s, \vec{r}) + \frac{v_0}{s + k_2}. \quad (15)$$

And for $r > w$

$$\bar{u}_>(s, \vec{r}) = \alpha_2(s) K_0(qr) \quad (16)$$

$$\bar{v}_>(s, \vec{r}) = \frac{k_1}{s + k_2} \bar{u}_>(s, \vec{r}) \quad (17)$$

where $\alpha_1(s)$ and $\alpha_2(s)$ are boundary matching parameters. They are functions of the Laplace transform variable s and are determined by matching the boundary conditions across $r = w$. At $r = w$, the continuity of the diffusion equation and their first derivatives imply

$$\bar{u}_<(s, w) = \bar{u}_>(s, w), \quad (18)$$

and

$$\bar{u}'_<(s, w) = \bar{u}'_>(s, w), \quad (19)$$

where $u'(s, w) = du(s, r)/dr$ at $r = w$. Insertion of the boundary conditions, Eqs. (18) and (19), in Eqs. (14) and (16) solves for α_1 and α_2

$$\alpha_1(s) = \frac{V}{q^2} \frac{1}{I_0(qw) + K_0(qw)I_1(qw)/K_1(qw)}, \quad (20)$$

and

$$\alpha_2(s) = \alpha_1(s) \frac{I_1(qw)}{K_1(qw)}. \quad (21)$$

Note that α_1 and α_2 are explicit functions of s . This is important in calculating the inverse transform of u and v .

The interaction / non-linear terms must be treated perturbatively because upon Laplace transformation they turn to a non-local integral in s . For example applying Laplace transform over u^2 turns into an integral equation with two interacting fields through a propagator

$$\int_0^\infty dt u^2(\vec{r}, t) e^{-st} = \frac{1}{(2\pi i)^2} \int_{-i\infty}^{i\infty} ds' \bar{u}(\vec{r}, s') \int_{-i\infty}^{i\infty} ds'' \bar{u}(\vec{r}, s'') \frac{\theta(s - s' - s'')}{s - s' - s''}. \quad (22)$$

In a weak non-linear coupling limit, we employ a perturbative approach to the non-linear terms in Eqs. (1 and 2)

$$\tilde{u} = u + u', \quad (23)$$

and

$$\tilde{v} = v, \quad (24)$$

where u and v are the solutions of the linear equations of Eqs. (1 and 2) where $k_3 = k_{12} = 0$. An equation for u_2 can be derived after substituting Eqs. (23 and 24) into Eqs. (1 and 2)

$$u' = -\frac{k_3 u^2}{k_1 + 2k_3 u} \quad (25)$$

B. Useful identities

Useful identities (see page 375, Eq. (9.6.15), Ref. [5])

$$I_\nu(z)K_{\nu+1}(z) + K_\nu(z)I_{\nu+1}(z) = \frac{1}{z}, \quad (26)$$

thus we find

$$I_0(qw)K_1(qw) + K_0(qw)I_1(qw) = \frac{1}{qw} \quad (27)$$

C. Fourier transform

Fourier transform

$$f(\omega) = \frac{1}{\sqrt{2\pi}} \int_{-\infty}^{\infty} dt f(t) e^{i\omega t} \quad (28)$$

Inverse Fourier transform

$$f(t) = \frac{1}{\sqrt{2\pi}} \int_{-\infty}^{\infty} d\omega f(\omega) e^{-i\omega t} \quad (29)$$

The following identity will be used for the inverse Laplace transform expression

$$f(t') = \frac{1}{2\pi} \int_{-\infty}^{\infty} d\omega e^{-i\omega t'} \int_{-\infty}^{\infty} dt e^{i\omega t} f(t) \quad (30)$$

The delta-function

$$\delta(t - t') = \frac{1}{\sqrt{2\pi}} \int_{-\infty}^{\infty} d\omega e^{-i\omega(t-t')} \quad (31)$$

$$\delta(\omega - \omega') = \frac{1}{\sqrt{2\pi}} \int_{-\infty}^{\infty} dt e^{i(\omega - \omega')t} \quad (32)$$

D. Laplace transform

Laplace transform

$$f(s) = \mathcal{L}[F(t)](s) = \int_0^\infty dt F(t) e^{-st} \quad (33)$$

Inverse Laplace Transform – Bromwich Integral

$$F(t) = \mathcal{L}^{-1}[f(s)](t) \quad (34)$$

We define (see page 908 in Ref. 6)

$$F(t) = e^{\gamma t} G(t) \quad (35)$$

Note $t \geq 0$. If $F(t)$ diverges as $e^{\alpha t}$, it is required γ to be greater than α . From Fourier transform, Eq.(30) we have ($t \rightarrow t'$ and $t' \rightarrow t$ and considering only a domain of positive time, $t \geq 0$):

$$G(t) = \frac{1}{2\pi} \int_{-\infty}^{\infty} d\omega e^{i\omega t} \int_0^\infty dt' e^{-i\omega t'} G(t'). \quad (36)$$

Introducing a complex variable $s = \gamma + i\omega$, and replacing $i\omega = s - \gamma$, and $ds = id\omega$ (assuming γ is a constant), in Eq.(36) we find

$$G(t) = \frac{1}{2\pi i} \int_{\gamma-i\infty}^{\gamma+i\infty} ds e^{(s-\gamma)t} \int_0^\infty dt' e^{-(s-\gamma)t'} G(t'). \quad (37)$$

Introducing $F(t) = e^{\gamma t} G(t)$

$$\begin{aligned} G(t) &= \frac{1}{2\pi i} \int_{\gamma-i\infty}^{\gamma+i\infty} ds e^{(s-\gamma)t} \int_0^\infty dt' e^{-st'} F(t') \\ &= \frac{1}{2\pi i} \int_{\gamma-i\infty}^{\gamma+i\infty} ds e^{(s-\gamma)t} f(s). \end{aligned} \quad (38)$$

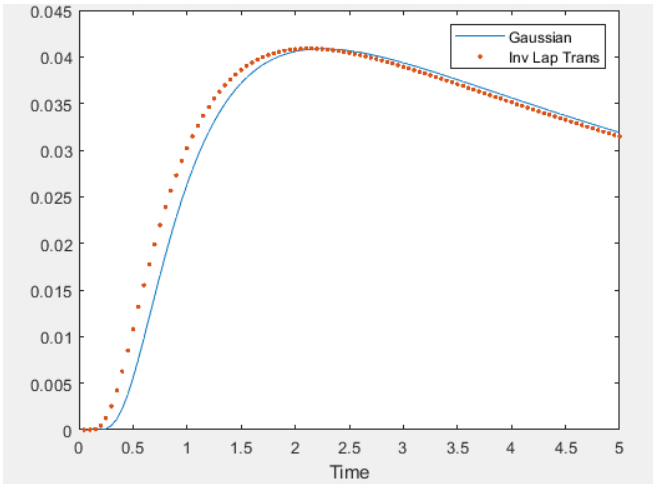


FIG. 1: Numerical solution of $u_{>}(\vec{r}, t)$ calculated by inverse Laplace transform (red dots) and a Gaussian function (solid line), given by Eq. (40), are shown. At large distances, i.e., $r \gg w$, the Gaussian is an approximate fit to $u_{>}(\vec{r}, t)$. The numerical values of the parameters used in the integration to produce this figure are $w = 1, r = 3, D_f = 1, k_1 = k_2 = k_3 = k_{12} = 0$.

Finally the integral expression for the inverse Laplace transform is given by

$$\begin{aligned} F(t) = G(t)e^{\gamma t} &= \frac{1}{2\pi i} \int_{\gamma-i\infty}^{\gamma+i\infty} ds e^{st} f(s) \\ &= \mathcal{L}^{-1}[f(s)](t). \end{aligned} \quad (39)$$

E. Appendix: Gaussian solutions

In the limit of ideal diffusion (in the absence of all reaction rates) the asymptotic solutions of $u_{>}(r, t)$ for large arguments, $r \gg w$, follow Gaussian distributions multiplied by the initial number of chemical species, $\pi w^2 u_0$

$$u_{>}(\vec{r}, t) = \frac{\pi w^2 u_0}{4\pi D_f t} e^{-\frac{r^2}{4D_f t}}. \quad (40)$$

This can be obtained from calculation of inverse Laplace transform of $u_{>}(s, r) = \alpha_2(s)K_0(q(s)r)$

$$\begin{aligned} \mathcal{L}^{-1}[u_{>}(qr)](t) &= \frac{1}{2\pi i} \int_{\gamma-i\infty}^{\gamma+i\infty} ds e^{st} u_{>}(s, r) \\ &= \frac{1}{2\pi i} \int_{\gamma-i\infty}^{\gamma+i\infty} ds e^{st} \alpha_2(s) K_0(q(s)r). \end{aligned} \quad (41)$$

Calculation of this integral requires numerical integration of Eq.(41), recalling the explicit dependence of α_2 and q on Laplace transform variable, s . We have performed this calculation and verified validity of Eq.(40) as illustrated in Fig. (1). In this figure, the numerical integration of the inverse Laplace transform of $u_{>}(\vec{r}, t)$, and fitting to a Gaussian PDF as given in Eq. (40) are plotted.

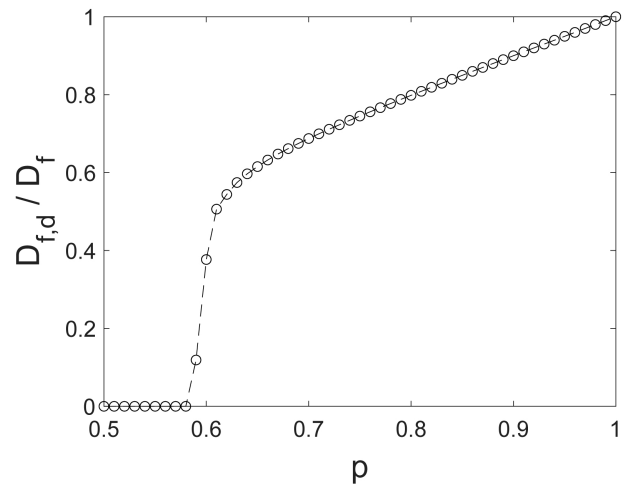


FIG. 2: Plot of the relative diffusion constant in a disordered ($D_{f,d}$) and ordered (D_f) square lattice as a function of p . By definition, D_f is the diffusion constant of a perfect lattice with $p = 1$. The ideal (ordered) square lattice consists of 500×500 sites. An abrupt transition in $D_{f,d}$ at the percolation threshold $p_c \approx 0.59$ is clearly seen.

F. Appendix: Random walk on a finite size disordered / porous system

In this subsection of the Appendix, we present a simplistic percolation model to calculate the diffusion constant in a disordered system as a function of site occupation probability, p , introduced in the main text. We formulate our computational approach to be consistent with the boundary conditions considered in this work, i.e., diffusive propagation of chemical species generated by passage of a particle in a super-cluster of connected points. Fig. 1 (in the main text) schematically presents a super-cluster, which consists of many smaller clusters. In the following, we reconstruct a model calculation for diffusion through a disordered / porous system based on the random walk on a two-dimensional lattice with lattice constant a .

Considering the time evolution of the diffusion front of a single track radially in a cylindrical geometry, we denote q and $1 - q$ the probabilities in taking a single step parallel and anti-parallel to \hat{r} , corresponding to outward and inward directions, respectively. We have assumed the radial motion in the absence of external torque (e.g., zero external magnetic field) and vortex flow of chemical species or scattering centers that convert the ideal system to disorder. Thus, although the present dynamical system looks effectively one-dimensional, it is inherently a two-dimensional problem. We therefore parameterize the net displacement relative to the center of the coordinate where the primary particle crosses perpendicularly (e.g., center of plane in Fig. 1 (in the main text)) with a single track in the middle), by $\vec{r} = ma\hat{r}$ in the limit of large displacements, $m \gg 1$. Here m is considered an integer number representing the net displacement steps

along the radial direction, \hat{r} .

The probability of finding the walker at displacement m after N -trials is given by the binomial distribution function

$$B_N(m) = \frac{N!}{\frac{N+m}{2}! \frac{N-m}{2}!} q^{\frac{N+m}{2}} (1-q)^{\frac{N-m}{2}}. \quad (42)$$

Hence, the first two statistical moments of the displacement can be calculated easily by $\bar{r} = a\bar{m} = aN(2q-1)$, and $\overline{r^2} = a^2\overline{m^2} = a^2(4Nq(1-q) + \bar{m}^2)$, thus $\Delta r = 2a\sqrt{Nq(1-q)}$ is the root-mean-square of the displacement. For an unbiased random walk, $q = 1/2$, hence $\bar{r} = 0$, $\overline{r^2} = Na^2$, and $\Delta r = a\sqrt{N}$. Considering t , the simulation time, $t \propto N$, we find $\Delta r \propto t^{1/2}$, where Δr increases indefinitely with time with the power-law exponent, $\beta = 1/2$, which is the hallmark of random growth.

Note that on a square lattice where we perform our computation to calculate the diffusion constant of a disordered system, where the cylindrical symmetry is broken down because of the presence of scattering centers and molecular heterogeneities, m splits into a pair of integer numbers: $m = (m_x, m_y)$, a vector in cartesian coordinates, representing the net displacement steps parallel to \hat{r} -direction. In this case, B_N in Eq. (42) would have been partitioned into products of two disjoint probabilities in terms of m_x and m_y . However, for simplicity and without loss of generality we disregard splitting B_N into two m_x and m_y components and consider m a single parameter (an integer number) that describes the dynamics of random walk.

As illustrated in Fig. 1, in the main text, (considering a single cylindrical track in the middle of the plane), a random walker starting from the middle of a discretized plane (the lattice) can reach the boundaries in a finite time. By taking a large number of steps, $N \gg 1$, the binomial probability, Eq. (42) can be approximated with a symmetric Gaussian distribution function

$$B_N(m) \approx B_N(\bar{m}) \exp\left(-\frac{(m-\bar{m})^2}{2Nq(1-q)}\right). \quad (43)$$

Considering an unbiased random walk with a single step probability $q = 1/2$, hence $\bar{m} = 0$, we simplify Eq. (43). In terms of continuous radial displacement, $r = ma$, we transform $B_N(m)$ in Eq. (43) to a normalized diffusion equation identical to the distribution function, given by Eq. (3), in the main text

$$B_N(r) = \frac{1}{4\pi D_f t} \exp\left(-\frac{r^2}{4\pi D_f t}\right). \quad (44)$$

Here $Na^2/4 = 2\pi D_f t$ where the simulation time, t , is proportional to the total number of trials / steps, N . Equivalently we identify expressions for the diffusion constant, $D_f = Na^2/(8\pi t)$, and the diffusion length, $\ell = a\sqrt{N/4\pi}$ using Einstein's relation, $\ell = \sqrt{2D_f t}$.

The random walker can reach the boundaries of the system if the following condition $\ell = L = r = ma$

is satisfied. Here L represents the finite dimension of the system / super-cluster. Transforming this condition to an equivalent condition for the diffusion constant, $D_f = \ell^2/2t = L^2/2t$, reveals linear proportionality of D_f to the planar area, L^2 and the number of points covering the area, connecting the center of coordinates to the boundaries which can be calculated simply by $(L/a)^2 = \pi N_r^2$ where N_r is number of radial points. In cartesian coordinates analogue of Eq.(44), $(L/a)^2 = N_x \times N_y$ where N_x and N_y are the number of points spanning along the x and y axis.

In a d -dimensional disordered system, where the molecular heterogeneities behave effectively like scattering centers, some of the lattice points randomly block the diffusion channels with probability p . Excluding the heterogeneity volumes (holes in Fig. 1 (in the main text) from the embedding volume, L^d , effectively lowers the diffusive volume, L^d , to L^f with $f < d$, the fractal dimension of the disordered / porous system. In our planar geometry, $d = 2$ is the dimension of Euclidian space embedding the disordered / porous surface with fractal dimension, $f < 2$ that is a function of p .

Thus the diffusion constant in the disordered system, $D_{f,d}$, can be expressed linearly proportional to D_f multiplied by a scaling factor, $L^{f-d} < 1$. More explicitly, $D_{f,d}/D_f = L^f/L^d$. In computational modeling of percolation theory, it is convenient to calculate L^f/L^d through a probability, $P(p, L) = N_p/(L/a)^2$, where N_p is the number of occupied points (with occupation probability p) enclosed by the boundaries of clusters subjected to a constraint that the boundaries of the clusters reach the boundaries of super-clusters. $P(p, L)$ can be interpreted as the probability of a single site to belong to a percolating cluster. The lower p , the lower $P(p, L)$ and $D_{f,d}$, hence the higher number of steps (simulation time) a random walker must take to cross the super-cluster. $P(p, L)$ continuously drops to zero as a function of p . In the vicinity of the percolation threshold, $p = p_c$, below which there would be no clusters connecting the opposite boundaries of the super-cluster, $P(p, L)$ and $D_{f,d}$ vanish simultaneously. This explicitly implies a lower diffusion constant in a disordered system relative to a perfect system as a function of p . As shown in Fig. 2, $D_{f,d}/D_f$ decreases with decreasing p and drops abruptly to zero below $p_c \approx 0.59$ for a 500×500 square lattice. For the two-dimensional system illustrated here it has been shown that in an infinite lattice the percolation threshold is $p_c = 0.5927$ [7]. To generate Fig. 2 we have developed an in-house code using image processing toolbox in matlab.

At $p = 1$ there is only one percolating cluster, identical to the super-cluster with $V = L^d$, volume of a d -dimensional hypercube. With a decrease in p , the population of non-percolating clusters and voids among clusters increases. It would be useful to partition the total volume, V , into volumes enclosed by the boundaries of percolating clusters, V_p , non-percolating clusters, V_{np} , and the volume of empty space (voids), V_e . Thus

$V = V_p + V_{np} + V_e$. In non-percolating clusters, a limited diffusion can be anticipated only within a finite size spanning over the size of non-percolating clusters, compared to unlimited diffusion length at the limit of large systems, i.e., $L \rightarrow \infty$, whereas V_e represents the volume of porous space through which the diffusion is forbidden.

We therefore express the probabilities in terms of fraction of these volumes. For example, $p = (V_p + V_{np})/V$ and $1-p = V_e/V$ represent fractions of occupied and unoccupied sites in an ensemble of clusters, sampled out of a pool of random copies and various site-configurations of a super-cluster. Similarly, a fraction of percolating volume yields $P(p, L) = V_p/V = L^f/L^d$.

G. Appendix: Ensemble average and restoration of translational and rotational symmetries

The underlying symmetries of the diffusion equation in a uniform medium exhibits translational and rotational invariance. The solutions, e.g., two-dimensional Gaussians, are cylindrically symmetric, as calculated in this Appendix and depicted in Fig. 1. In the presence of random scattering centers, the system is disordered, and translational and rotational symmetries are violated. The Gaussian distribution functions are no longer solutions of the stochastic partial differential equations where the diffusion constant varies randomly as a function of position. In a specific random copy of a disordered system, one needs to calculate the solutions of the stochastic diffusion equation numerically, prior to performing ensemble averaging over various copies of random scattering centers, as we have performed and discussed in Fig. 2.

In percolation theory, Sec. IG, we have introduced an

approach and calculated the mean diffusion constant by $D_{f,d}/D_f = P(L, p)$. Because $P(L, p)$ is the probability of percolating clusters, it represents volumes of percolating clusters over the volume of a super-cluster (L^d) in an statistical sense. It has been calculated by counting the number of points encompassed within a closed-loop constructed out of the boundaries of a specific percolating cluster, averaged over all percolating clusters. Thus, as shown in Fig. 2, $D_{f,d}$ represents a scalar that is only a function of p . All details of exact positions on the scattering centers are washed out, hence, there is no spatial dependence on the position of the scattering sites on $D_{f,d}$, simply because we have performed an averaging over random copies of scattering center positions.

Substituting $D_{f,d}$ for D_f in the standard diffusion equation, naturally, restores cylindrical symmetries because the disorders effectively renormalize the value of the diffusion constant by a scaling factor. In Fig. 2 (in the main text), we have calculated localized solutions of diffusion equation, with no cylindrical symmetries, considering only one copy of randomness in scattering center positions, embedded in $D_{f,d} = D_f(\vec{r})$.

The differences in local and global characters of the solutions, such as the (Anderson) localization of the solutions, stem from the steps in which ensemble averaging has been performed, before or after calculating the solutions, as these two operations are non-commutative: (1) calculating numerical solutions of the diffusion equation assuming $D_{f,d} = D_f(\vec{r})$ and (2) performing ensemble average over the percolating clusters (loops) and tracing out locations of the scattering centers.

Depending on which of these approaches are relevant to the physical system under investigation, we may arrive to drastically different conclusions for the intra- vs. inter-track couplings at FLASH UHDR.

-
- ¹ R. Abolfath, D. Grosshans, R. Mohan, *Oxygen depletion in FLASH ultra-high-dose-rate radiotherapy: A molecular dynamics simulation*, Med. Phys. **47**, 6551-6561 (2020).
 - ² J. Schuemann, A. L. McNamara, J. Ramos-Mendez, *et al.*, *TOPAS-nBio: an extension to the TOPAS simulation toolkit for cellular and sub-cellular radiobiology*. Radiat. Res. **191**, 125–138 (2019).
 - ³ A. Baikalov, R. Abolfath, R. Mohan, E. Schüler, J. J. Wilkens, S. Bartsch1, *An analytical model of intertrack interaction at ultra-high dose rates and its relevance to the FLASH effect*, submitted to Med. Phys. (2022).
 - ⁴ H. S. Carslaw, J. C. Jaeger, *The Laplace transformation: problems on the cylinder and sphere. Composite cylindrical regions. In Conduction of Heat in Solids*. Oxford University Press, New York. 345–347 (1959).
 - ⁵ M. Abramowitz and I. A. Stegun, *Handbook of Mathematical Functions*, Dover publisher (1964).
 - ⁶ G. B. Arfken, H. J. Weber, *Mathematical methods for physicists*, 4th Edition, Academic Press, (1995).
 - ⁷ D. Stauffer, A. Aharony, *Introduction To Percolation Theory*, Taylor & Francis; 2nd edition.